

24 **Abstract**

25 Our understanding of *in situ* microbial physiology is primarily based on physiological
26 characterization of fast-growing and readily-isolatable microbes. Microbial enrichments to obtain
27 novel isolates with slower growth rates or physiologies adapted to low nutrient environments are
28 plagued by intrinsic biases for fastest-growing species when using standard laboratory isolation
29 protocols. New cultivation tools to minimize these biases and enrich for less well-studied taxa are
30 needed. In this study, we developed a high-throughput bacterial enrichment platform based on
31 single cell encapsulation and growth within double emulsions (GrowMiDE). We showed that
32 GrowMiDE can cultivate many different microorganisms and enrich for novel taxa that are never
33 observed in traditional batch enrichments. For example, preventing dominance of the enrichment
34 by fast-growing microbes due to nutrient privatization within the double emulsion droplets allowed
35 cultivation of novel *Negativicutes* and *Methanobacteria* from stool samples in rich media
36 enrichment cultures. In competition experiments between growth rate and growth yield specialist
37 strains, GrowMiDE enrichments prevented competition for shared nutrient pools and enriched for
38 slower-growing but more efficient strains. Finally, we demonstrated the compatibility of
39 GrowMiDE with commercial fluorescence-activated cell sorting (FACS) to obtain isolates from
40 GrowMiDE enrichments. Together, GrowMiDE + DE-FACS is a promising new high-throughput
41 enrichment platform that can be easily applied to diverse microbial enrichments or screens.

42

43 **Introduction**

44 Microbial physiology is largely based on studies using microbes isolated in pure cultures.
45 Techniques for isolating novel microbes for the last 140 years involve recreating a favorable

46 environment and flux of nutrients in the laboratory that mimics natural conditions and then
47 attempting to recover the grown novel species. As a result, current methods are inherently biased
48 towards fast-growing microbes that can outcompete other species for shared nutrients, even species
49 with minor differences in maximal growth rate (μ_{Max}) (**Fig. S1-S3**)[1, 2]. The missing slower-
50 growing species might have unknown physiological strategies to adapt to their natural environment
51 and that likely play critical roles in community resilience [3]. For example, growth efficiency
52 (growth yield) over growth rates has been suggested as a survival strategy in low nutrient flux or
53 spatially-structured environments including biofilms[1, 2, 4] and the marine subsurface
54 environment (~30% of Earth's biomass)[5–8]. Therefore, there is a critical need to develop new
55 cultivation tools that minimize the bias for fast microbial growth rates.

56 Traditional methods that limit competition for finite resources (i.e., by nutrient
57 privatization) typically rely on spatial separation and include dilution-to-extinction or plating for
58 colony forming units[9, 10]. However, these techniques depend on cell abundances, are low-
59 throughput, and are not conducive to recovering microbes that grow poorly at air-liquid interfaces,
60 especially anaerobes. Droplet microfluidics approaches have emerged as a powerful high-
61 throughput technique to cultivate novel microorganisms in isolated bioreactors each with precise
62 distributions of reagents necessary for growth[10–14], facilitating screens for antibiotic
63 resistances[11, 15, 16], and measurements of cellular activity[17–19]. Most microbiological
64 droplet approaches use single emulsion droplets, in which aqueous droplets containing cells and
65 medium are suspended within an oil phase. Many studies have shown the utility of single emulsion
66 droplet microfluidics for surveying microbial diversity[19–22], obtaining high quality
67 genomes[23], and functional screens[10, 11, 14, 16]. Single emulsion enrichment techniques have
68 also demonstrated selection for strains that have elevated growth yields or slower growth rates,

69 serving as a proof-of-concept for the impact of nutrient privatization on enrichment outcomes[24].
70 However, single emulsion droplets require custom equipment to analyze downstream and have
71 only been sorted in proof-of-concept demonstrations with slow sorting speeds and limited
72 fluorescence channels[25, 26], making them challenging to apply to new systems.

73 Double emulsion droplets (DEs) are an innovative microfluidics platform with the potential
74 to greatly simplify microbial growth and isolations[27–30]. DEs consist of an inner aqueous
75 compartment surrounded by an oil shell suspended within an outer aqueous layer (**Fig. 1B**). The
76 outer aqueous suspension makes DEs directly compatible with common flow cytometry
77 equipment, allowing them to be sorted via fluorescence-gated sorting (FACS) similar to cells[31].
78 Recent work optimizing device design, surfactants and sorting parameters has advanced the ability
79 to sort DEs at high-throughput (12-14 kHz) and single droplet accuracy (>99% purity, 70% single
80 droplet recovery) in traditional FACS instruments[31, 32]. Current applications for DE technology
81 include cell encapsulation[19, 27], drug delivery[29], and protein function screens[19]. However,
82 DEs have not yet been used as an enrichment platform for microorganisms.

83 We designed a high-throughput DE platform (GrowMiDE) that i) is compatible with
84 diverse microbial physiologies, ii) facilitates enrichments and subsequent isolations for
85 downstream phenotypic characterizations, and iii) demonstrates recovery of microbial species that
86 are normally lost due to outcompetition in batch culture enrichments. The GrowMiDE platform
87 minimized bias for fast growth rates through nutrient privatization in individual droplets,
88 facilitating enrichment of slower-growing species. Using GrowMiDE, we demonstrated
89 enrichment of distinct community compositions compared to traditional batch cultures from the
90 human gut microbiome, including a 22-fold increase in a novel *Negativicutes* species from the
91 “most wanted” microbiome list[33]. We also determined that GrowMiDE can be applied to enrich

92 for novel taxa due to prioritization of traits other than fast growth rates, specifically higher growth
93 yields. Finally, we demonstrated the combination of GrowMiDE and DE-FACS as an isolation
94 tool for microbiologists. This platform can be readily adapted to diverse biological systems and
95 our results demonstrate the feasibility of high-throughput DE culturing to obtain cultured
96 representatives of overlooked physiologies.

97

98 **Materials and Methods**

99 Strains and growth conditions

100 *E. coli* MG1655 and *E. coli*-GFP were routinely cultivated on LB agar or M9 medium
101 supplemented with 25 mM glucose at 37°C with shaking. *Lactococcus lactis* spp *cremoris* WT
102 (NZ9000) and the derived mutant Δ *ldhA* (NZ9010)[24] were cultivated in 10 mL of chemically
103 defined medium (CDM)[34] supplemented with 1.5% casamino acids (w/v), 26 mg/L L-
104 tryptophan, and 50 mM glucose at 30°C. Starter cultures of NZ9000 or NZ9010 were inoculated
105 from a single colony from Difco M17 broth + 25 mM glucose (GM17) or GM17 + 5ug/mL
106 erythromycin plates, respectively. *Pseudomonas putida* were routinely cultivated on LB agar or
107 cetrimide plates. All growth curves were started with a 1% inoculum from a starter culture in
108 stationary phase. For culturing strict anaerobes in DEs, 20 mL stationary cultures grown in
109 anaerobic 60 mL serum vials were used as the inocula. *Desulfovibrio ferrophilus* IS5 (DSM no.
110 15579) was cultivated at 30°C in modified artificial seawater medium[35] supplemented with 60
111 mM lactate and 30 mM sulfate. *Thermoanaerobacter kivui* TKV002 was grown at 65°C in medium
112 containing 25 mM MES (free acid), 75 mM MES (sodium salt), 13.7 mM NaCl, 0.8 mM MgSO₄,
113 18.7 mM NH₄Cl, 1.3 mM KCl, 0.1 mM CaCl₂, 0.7 mM KH₂PO₄, 40 μM uracil, 1 mL/L trace

114 element solution SL10, 1 mL/L selenate-tungstate solution, 1 mM Na₂S, 0.5 mg/L resazurin, and
115 50 mM glucose as the catabolic substrate in DEs. Stool enrichments were grown at 37°C cultivated
116 in modified mBHI medium containing: 37 g/L BHI mix (RPI), 200 mg/L tryptophan, 1 g/L
117 arginine, 5 mg/mL menadione, 500 mg/L cysteine HCl, 0.12 µg/mL haemin solution[36], 0.2 g/L
118 mucin, resazurin. For select enrichments, mBHI was supplemented with additional media
119 components (mBHI⁺) based approximately on concentrations added to Gut Microbiota Medium
120 (GMM)[36]: 3 mM sugars (glucose, cellobiose, maltose, fructose), 30 mM sodium acetate, 8 mM
121 propionic acid, 4 mM sodium butyrate, 15 mM sodium lactate, 30 mM NaHCO₃.

122 Analytical procedures

123 Cell densities were determined based on the optical density at 600 nm (OD₆₀₀) using an
124 Ultraspec 2100 spectrophotometer (GE Healthcare) or a Tecan Infinite M1000 microplate reader.
125 Glucose and fermentation profiles of *L. lactis* strains were quantified using an Agilent 1260
126 Infinity high-performance liquid chromatograph as described previously[37]. For *L. lactis*
127 competition experiments, colony forming units were measured on GM17 (NZ9000 + NZ9010) or
128 GM17 + 5µg/mL erythromycin (NZ9010 only) plates. Microscopy analysis was performed on a
129 Leica DM4000B-M fluorescence microscope using standard brightfield and FITC filter settings.

130 Double emulsion generation

131 The Dropception setup consists of four syringe pumps for the carrier phases (Harvard Apparatus
132 PicoPlus Elite), a stereoscope (Amscope), a high-speed camera (ASI 174MM, ZWO), and a
133 desktop computer (HP). Consumables included PE-2 tubing, eppendorf or anaerobic vials for
134 droplet collection, media components, and HFE7500 oil + 2.2% Ionic Krytox (FSH, Miller-
135 Stephenson)[38]. The cell and inner phases for the aqueous droplet cores typically contained basal

136 bacteria growth medium (LB, M9, CDM, mBHI), 0.5 % BSA, and any indicated catabolic
137 substrates or dyes. 10% Optiprep (Sigma) was added to the cell phase as a density modifier to
138 ensure equal relative flow rates between the inner and cell phases during live DE generation. Cells
139 were diluted to an $OD_{600} = 0.05$ in the cell carrier phase for single-cell loading (~20% of DEs
140 contain a single cell, ~2% of DEs contain 2 cells) based on a Poisson distribution. The outer
141 aqueous carrier phases contained matching bacterial growth media to the aqueous core, 2%
142 Pluronic F68 (Kolliphor P188, Sigma), and 1% Tween-20 (Sigma). For anaerobic enrichments, all
143 components were assembled inside an anaerobic chamber (COY), and all consumables were left
144 in the anaerobic chamber to remove excess oxygen at least 3 days prior to use. Dropception device
145 master molds for 30 and 45 μm DEs were designed in AutoCAD 2019 and fabricated via multilayer
146 photolithography in a clean room as described previously[31]. Dropception PDMS devices were
147 made through standard one-layer soft lithography on a standard laboratory benchtop as described
148 previously[31]. Immediately prior to use, the outer and outlet channels of the PDMS devices were
149 selectively O_2 plasma treated for 12 minutes at 150 W in a Harrick PDC-001 plasma cleaner,
150 flushed with PBS + 2% Pluronic F68, taped with scotch tape, and transferred into the anaerobic
151 chamber or aerobic setup. The four phases (oil, cell, inner, outer) were loaded into syringes
152 (PlastiPak, BD) and connected to the device via PE/2 tubing (Scientific Commodities). Typical
153 flow rates were 300:100:105:6000 (oil : cell : inner : outer) $\mu\text{L h}^{-1}$ for dual-inlet 45 μm devices
154 and 275:85:2500 (oil : inner : outer) $\mu\text{L h}^{-1}$ for single-inlet 30 μm devices. Live DE generation
155 was monitored using the stereoscope and high-speed camera inside the anaerobic chamber.

156 DE-FACS

157 DE-FACS was performed as previously described on a Sony SH800 [27, 31]. Briefly, 50 μL of
158 DEs were diluted into 500 μL of FACS diluent buffer (PBS + 1% Tween-20) in a 5 mL 12 x 75

159 mm round bottom FACS tube (BD Biosciences). After standard autocalibration on the Sony
160 SH800, the DEs were gently resuspended prior to loading, and the droplets were analyzed on a
161 130 μm microfluidic chip using a standard 408 nm laser configuration. DEs appear on the SH800
162 after 2 - 3 minutes within specific FSC-H and FSF-W gates, followed by subsequent gating on
163 FITC fluorescence when indicated for sorting (yield mode). Drop delay adjustments for sorting
164 were manually calibrated as described previously[31]; optimal drop delay settings typically
165 matched those estimated by the autocalibrated Sony SH800 settings to achieve >50% DE recovery
166 in 96 well plates for 30 μm DEs. Event rates for FACS analysis were kept below 1000 events/s
167 and sorting rates were maintained under 50 events/s. Gain settings for DE-FACS were described
168 previously[31], with the exception of the FITC gain, which was set to 32% or 40% for *E. coli* GFP
169 or SYTO-stained cells, respectively. Sorted DEs were deposited into either FACS tubes or 96 well
170 plates pre-loaded with 100 μL of osmolarically-balanced outer solution based on inner core media
171 components. Sorted DE populations were imaged on a Leica DM4000B-M fluorescence
172 microscope and a Leica DM E brightfield microscope.

173 Mathematical modeling

174 The mathematical models used to simulate competitive outcomes of rate vs yield specialists was
175 based on previous Monod models [39, 40], except the dilution term was removed to reflect
176 growth in fed-batch cultures and the growth kinetic parameters were based on experimentally-
177 determined monoculture growth trends collected previously [24] and within this study.
178 Differential equations used in the basal model and extended discussions are included in the
179 supplemental data.

180 MATLAB code

181 The MATLAB program was customized to analyze Leica DM4000B-M fluorescence microscope
182 images (TIFF format) with the standard brightfield and FITC filter settings overlaid (F1C).
183 MATLAB first processed each image by sharpening droplet edges, identifying each droplet's
184 coordinates via the *findcircles* function, and cropping around each droplet. Then, it overlaid a
185 white, circular mask sized with each droplet's radii so that only the pixels inside the droplet were
186 included in the image crop. The radii of the white masks were adjusted to remove the excess droplet
187 edge boundaries (SF5). Then the code summed all pixel intensities above an experimentally
188 determined threshold (data not shown) inside the droplet interior. This threshold was implemented
189 to remove excess black pixels so that larger droplets did not return higher summed pixel intensities.
190 The program ultimately returned a table with all indexed droplets and their respective fluorescence
191 sums, which was then analyzed to relate number of cells to fluorescence.

192 16S sequencing

193 16S sequencing was performed and analyzed by the ZymoBIOMICS Service (Zymo Research,
194 Irvine, CA). Zymo Research performed library preparation, post-library QC, sequencing using a
195 Illumina MiSeq Platform, and bioinformatics analysis using the Dada2 and QIIME pipeline. Raw
196 reads and metadata were submitted to SRA under BioProject PRJNA852267.

197

198 **Results**

199 **Development of GrowMiDE platform for microbial enrichments**

200 To encapsulate single microbial cells for parallel high-throughput culturing in DEs, we
201 based GrowMiDE on the Dropception[31] microfluidic platform, which consists of a simple one-
202 step microfluidic device, syringe pumps for the carrier phases, a high-speed camera, and a

203 stereoscope (**Fig. 1A, Fig. S4**). Monodisperse DEs of 30 or 45 μm in total diameter, respectively
204 dependent on device geometry, were generated at ~ 1 kHz containing: HFE7500 + 2.2% ionic
205 Krytox[38] as the oil phase, basal growth medium + 2% pluronix F68 + 1% Tween-20 as the outer
206 phase, and PBS or basal growth medium + 0.5% BSA + catabolic substrates as the cell and inner
207 phases, respectively (**Fig. 1A,B**). After generating DEs within the microfluidic device, we
208 collected them in bulk for downstream incubation or analysis (**Fig. 1B**). To ensure DEs contained
209 only a single cell after stochastic loading, we operated within a Poisson regime in which 80% of
210 DEs were empty and 98% of the DEs containing cells contained only a single cell (OD_{600} 0.05 in
211 cell carrier phase). Collecting DEs for 4 hours yielded ~ 48 million parallel DE microreactor
212 cultures containing single cells, allowing for an increased encapsulation of low-abundance species.

213 To determine if single cells encapsulated in DEs would grow, all DEs were incubated in
214 bulk and microbial growth in droplets was assessed by brightfield or fluorescence microscopy
215 (**Fig. 1C,D**). Overnight incubation of DEs containing single *Escherichia coli* cells constitutively
216 expressing GFP resulted in DEs containing 30-100 cells (~ 5 -7 generations), indicating robust
217 growth in droplets uninhibited by DE components (**Fig. 1C**). GrowMiDE is compatible with both
218 aerobic and anaerobic microbial growth; the Dropception setup is fully operable within an
219 anaerobic glove box (**Fig. S4**). To demonstrate these capabilities, we successfully encapsulated
220 and grew several facultative and strictly anaerobic microbes including *E. coli* MG1655
221 (performing mixed acid fermentation), *Lactococcus lactis spp cremoris* NZ9000 (lactic acid-
222 producing fermentation), *Desulfovibrio ferrophilus* IS5 (sulfate reduction) and the thermophile
223 *Thermoanaerobacter kivui* (acetogenesis at 65°C) (**Fig. 1D**). These results establish that DEs are
224 a suitable high-throughput platform to cultivate diverse microbial species.

225 To quantify growth in DEs, we developed a custom MATLAB script to automatically
226 detect per-droplet intensities from fluorescence microscopy images (**Fig. S5, S6**). Using GFP-
227 expressing *E. coli* and this automated script, we analyzed growth in DEs containing either glucose
228 or acetate in the inner phase as the sole catabolic substrates (**Fig. S7A**). Net *E. coli*-GFP growth in
229 DEs matched batch cultures (**Fig. S7B,C,D**), indicating that *E. coli* growth in GrowMiDE and
230 batch cultures are comparable. Together, these data demonstrate that the GrowMiDE platform can
231 be used to cultivate and quantify growth of diverse microbial species in high-throughput.

232

233 **GrowMiDE enriches for microbial communities distinct from traditional batch cultivation**

234 We next used the GrowMiDE platform to cultivate cells from a mixed microbial
235 community. We focused specifically on the human gut microbiome due to knowledge of major
236 metabolic groups of microorganisms[41–44] and established media conditions that can cultivate
237 many different taxa[33, 45]. Specifically, we tested whether GrowMiDE cultivation enriched for
238 novel taxa by comparing microbial enrichments performed in either batch cultures or DEs (**Fig.**
239 **2A**) (**Table S2**). 16S rRNA gene sequencing revealed a clearly distinct microbial community
240 composition in GrowMiDE enrichments relative to batch-grown cells, even in the same basal
241 medium (mBHI) (**Fig. 2B**). While the absolute number of recovered species did not differ
242 significantly between batch and GrowMiDE enrichments (**Fig. 2C**), the unique identities of
243 enriched ASVs were significantly different (**Fig. 2D**). Interestingly, GrowMiDE uniquely yielded
244 significant growth ($6.0 \pm 4.0\%$, SD, 4/6 replicates) of the gut hydrogenotrophic methanogen
245 *Methanobrevibacter smithii*, enriched from $\sim 0.4\%$ in the corresponding input stool community
246 (**Fig. 2B, Fig. S8A,C**). The most surprising increase of a single taxa in GrowMiDE enrichments
247 was the enrichment of the Negativicutes *Phascolarctobacterium faecium* ($17.8 \pm 9.8\%$, SD, 6/6

248 replicates), a 22-fold increase from the relative abundance in the input stool community ($0.8 \pm$
249 0.2% , SD, $n=5$). (**Fig. 2B, Fig. S8B,D**). Negativicutes are a poorly understood phylogenetic group
250 with a unique cell envelope structure, and they are thought to play a role in production of critical
251 short chain fatty acids (SCFA) in the gut microbiome[46, 47]. The *in situ* metabolism of *P. faecium*
252 is unknown, but its primary catabolism is thought to be secondary fermentation (succinate to
253 propionate)[48]. *P. faecium* has been suggested to participate in vitamin B₁₂ cross-feeding with
254 *Bacteroidetes*[49]. Strikingly, *P. faecium* is present in over 67% of human stool samples[46],
255 however, it is difficult to isolate and, therefore, was featured on the Human Microbiome Project's
256 "Most Wanted" list[33].

257 In batch cultures, the final microbial composition was mostly established within 12 hours,
258 consistent with growth dominated by the fastest species in an artificial laboratory environment (eg
259 *E. coli* and *Enterococcus spp.*) (**Fig. 2E**). However, in GrowMiDE enrichments we observed
260 gradual enrichment and increased gene copies of *M. smithii* and *P. faecium* over time (**Fig. 2E-G**).
261 The appearance of these taxa at later timepoints and their enrichment across time support the
262 hypothesis that the GrowMiDE platform decreased the bias against slower-growing species and
263 facilitated enrichment of novel physiologies, even with non-selective medium.

264

265 **GrowMiDE favors growth yield specialists over growth rate specialists**

266 We hypothesized that stool GrowMiDE cultures enriched for slower-growing taxa by
267 minimizing competition for shared nutrients between droplets (i.e. nutrient privatization). Nutrient
268 privatization through spatial structuring promotes diversity in communities, including microbes
269 that prioritize growth yield over rate that would otherwise be lost in laboratory enrichments (**Fig.**
270 **S1C**). Trade-offs between rate and yield-specialists has been well-documented in *Lactococcus*

271 *lactis* strains[24, 34](**Fig. 3A**). Under high glucose flux conditions, wild type *L. lactis* (NZ9000)
272 ferments 1 mol glucose to 2 mol lactate by homofermentative lactic acid fermentation (**Fig. S2A**),
273 resulting in a net yield of 2 mol ATP per mol glucose. Under conditions of low glucose flux,
274 fermentation shifts towards formation of ethanol and acetate (**Fig. S2B**), resulting in a total net
275 gain of 3 mol ATP per mol glucose. This latter fermentative metabolism is locked in a *L. lactis*
276 lactate dehydrogenase deletion mutant ($\Delta ldhA$, NZ9010). Although the $\Delta ldhA$ strain has a higher
277 growth yield, it comes at a trade-off in a reduction of the maximum growth rate (**Fig. 2B**). In
278 elegant single emulsion experiments, encapsulation of WT and $\Delta ldhA$ strains resulted in
279 enrichment of the efficient, but slower-growing $\Delta ldhA$ strain across transfers[24].

280 To test whether DEs similarly maintained populations with higher growth yield, we
281 competed *L. lactis* WT and $\Delta ldhA$ strains in batch vs GrowMiDE enrichments over serial transfers.
282 Growth rates of batch cocultures containing a 1:1 mixture of both strains resembled the faster WT
283 strain (**Fig. 3B**), which was consistent with WT constituting over 80% of the culture after transfer
284 0 (**Fig. 3C**). As expected, even when the $\Delta ldhA$ strain was inoculated at a high frequency of 80%,
285 it was outcompeted to less than 0.003% by WT within 2 transfers in batch culture (**Fig. 3C**)[24].
286 In contrast, the slower $\Delta ldhA$ population was maintained and even dominated WT in GrowMiDE
287 enrichments across transfers (99.33% $\Delta ldhA$ by transfer 4) (**Fig. 3D**), showing that GrowMiDE
288 can retain or even enrich slower-growing species from mixed communities through nutrient
289 privatization.

290

291

292 **GrowMiDE + DE-FACS as a high-throughput enrichment and isolation tool**

293 A useful feature of DE platforms is direct compatibility with traditional microscopy or
294 FACS (DE-FACS) (**Fig. 4A**) [31, 32, 50, 51]. Developing a platform that facilitates high-
295 throughput encapsulation and the ability to selectively isolate droplets of interest has broad
296 applications including improved genome recovery[52], antimicrobial sensitivity assays[16, 53],
297 and directed evolution studies[54]. To test whether our cell-containing DEs could be accurately
298 distinguished and isolated from empty DEs via fluorescence during FACS, we encapsulated and
299 grew *E. coli* cells expressing GFP in DEs and then attempted to isolate only cell-containing
300 droplets via FACS. Distinct FACS populations of empty and cell-laden DEs were observed by
301 FACS, and fluorescent microscopy measurements confirmed that 97.5% of the sorted positive
302 population contained intact DEs loaded with cells (**Fig. S9A**). We also assessed whether DE-FACS
303 can differentiate between empty and microbe-containing DEs by adding a fluorescent dye
304 (SYTO_{bc}) during cell encapsulation. We identified FACS gates that distinguished empty DEs from
305 DEs containing *E. coli* MG1655 loaded with 2.5 μ M SYTO_{bc} grown for 24 hours (**Fig. S9B**).
306 Within the SYTO⁺ DE population, 92.2% contained cells as confirmed by brightfield microscopy
307 based on detecting cell motility. Longer incubation times decreased fluorescence signal; however,
308 SYTO⁺ DE populations were still detectable at 48 hours (**Fig. 4C**). Relative to the input
309 GrowMiDE enrichment that contained ~80% empty DEs, DE-FACS resulted in a 443- and 419-
310 fold enrichment for DEs containing *E.coli*-GFP and *E.coli* + SYTO_{bc} DEs, respectively. These
311 results demonstrate the application of DE-FACS to sort for DE droplets containing grown bacterial
312 cells.

313 A major barrier in single emulsion microfluidics and traditional single-cell FACS sorting
314 is the difficulty in isolating live cells for downstream phenotypic analysis. While single-cell
315 genomes can easily be recovered in downstream processes even if cells die, preserving cell

316 viability in sorted populations is essential for downstream characterization of microbial
317 physiology. High-throughput microbial cultivation using GrowMiDE and isolations using DE-
318 FACS therefore has the potential to be a powerful approach for screens, enrichments, and
319 isolations (**Fig 4A**). As a proof of concept, we demonstrated the application of GrowMiDE + DE-
320 FACS in a synthetic glucose-catabolizing community containing *E. coli*, *Pseudomonas putida*, *L.*
321 *lactis* WT, and *L. lactis* Δ *ldhA*. The synthetic community was chosen due to i) compatibility of all
322 species in a defined medium, ii) a comparable catabolic usage of glucose, and iii) the ability to use
323 selective plating to phenotypically assess species identities from mixed cultures. *E. coli* dominated
324 both batch and GrowMiDE enrichments due to higher relative growth rate and yields in pure
325 cultures (**Fig. S10**); however, only GrowMiDE cultivation preserved all 4 strains in the synthetic
326 community (**Fig. 4B, Fig. S11**). Illustrating how even minor decreases in maximal growth rates
327 can drive species lost in batch cultures, *P. putida* was frequently lost in batch culture competitions
328 after 48 hours despite having the second highest growth rate and yield in monocultures (**Fig. S10**).
329 For GrowMiDE enrichments, we sorted individual DEs from the SYTO⁺ DE population (**Fig. 4C**)
330 into 96 well plates, released encapsulated clonal populations from DEs with PFO, and collected
331 growth measurements of recovered isolates. Here, we used 48 hour incubations despite decreased
332 stained bacterial intensities and resulting broader FACS gates to provide sufficient time for all
333 strains to grow in DEs (**Fig. 4C, Fig. S10**). Our approach included dimly-fluorescent DEs to limit
334 bias in staining efficiency between different species with the trade-off of sorting a higher fraction
335 of empty DEs (**Fig. 4C**). Across two 96-well plate arrays, 77 wells contained bacteria recovered
336 from sorted DEs, 73 (95%) of which were confirmed to be pure cultures by selective plating for
337 all 4 input species (**Fig. 4D**). Consistent with the 2 dominant species abundances from GrowMiDE
338 enrichments (87% *E. coli* : 12% *P. putida*), 79% of the recovered pure cultures were *E. coli* and

339 16% were *P. putida*. Together, these results demonstrate the feasibility of microbial enrichments
340 and isolations using GrowMiDE + DE-FACS.

341

342 **Discussion**

343 Here, we demonstrated a novel application of DE technology to cultivate microbes and
344 perform high-throughput enrichments for slower-growing microbes in both defined and undefined
345 communities. We demonstrated that many metabolically diverse microbial species can grow in
346 GrowMiDE, including strict anaerobes (**Fig. 1**). Moreover, GrowMiDE can also facilitate
347 enrichment for microbes pursuing a growth yield over growth rate strategy (**Fig. 3D**). GrowMiDE
348 enrichments uniquely yielded microbial species that were never observed in batch culture using
349 the same enrichment medium (**Figs. 2,4**). Finally, we demonstrated the application of GrowMiDE
350 and DE-FACS as a platform to obtain isolates for downstream characterization and physiological
351 studies (**Fig. 4**).

352 In our study, nutrient privatization allowed slow-growing species to escape competition [1,
353 2]. Although DEs spatially separate cells and large macromolecules in separate microreactors, the
354 inner aqueous core is only separated from the environment by a thin oil shell. Dependent on the
355 local surfactants and blocking agents used in the oil layer, DEs can therefore be selectively
356 permeable to small molecules including oxygen, salts, and some dyes[28–30, 55]. This effect is
357 reported to be tunable dependent on surfactant properties and concentrations[55]. Other
358 rheological studies in DEs have also shown that rhodamine A, BSA conjugates, and
359 anhydrotetracycline can traffic across the oil shell in a pH-mediated delivery system in some DE

360 formulations[29]. The molecular mechanism of crossover is unknown, although facilitated
361 diffusion and spontaneous emulsification have been hypothesized[29, 56].

362 While it is possible that low levels of carbon source crossover occurred within our
363 GrowMiDE enrichments, the levels of glucose retained within the DEs remained sufficient to favor
364 growth of slow-growing *L. lactis* Δ *ldhA* mutants (**Fig. 3D**). Degrees of nutrient privatization can
365 be dynamic; even partial privatization, in which limited competition exists, can be sufficient to
366 preserve distinct populations[57–59]. Another possibility is that low permeability of DEs for
367 certain compounds could have facilitated the growth of *M. smithii* and/or *P. faecium*. *P. faecium*
368 and *M. smithii* have been indicated to be fully dependent on cross-fed metabolites from the gut
369 community, succinate and H₂ respectively; however, neither compound was added to the
370 GrowMiDE enrichments. H₂ is produced during fermentation by many co-enriched gut species
371 and should readily diffuse across the HFE7500 oil. For *P. faecium* enrichments, it is unclear how
372 picomolar concentrations of succinate crossover from a subsection of a mixed community would
373 promote a significant enrichment. Full genome sequence analysis of the two existing isolated *P.*
374 *faecium* strains suggests that fermentation of succinate to propionate is their only primary
375 catabolism[60]. However, it is possible that the GrowMiDE enrichment facilitated the use of other
376 catabolic substrates that were available in our enrichments, either in the basal mBHI medium or
377 produced by another species. Control batch culture enrichments supplemented with DE
378 components did not enrich for *P. faecium* (data not shown), ruling out the possibility of catabolism
379 of oil or DE surfactants.

380 Recent advances in microfluidic technology to expand the number of cultured species
381 include custom devices to isolate and incubate single cells (iChip, SlipChip)[61–63] and
382 culturomics, in which bacterial colonies are arrayed across media conditions on plates and

383 identified using MALDI-TOF[45]. However, these technologies are limited in throughput and
384 require specialized, expensive equipment to analyze and sort grown cultures. The GrowMiDE
385 platform is highly amenable to diverse applications and requires only simple instrumentation, all
386 of which can be assembled and operated with minimal training. In this study, we showed that
387 GrowMiDE eliminated competition with faster growing microbes and enriched microbes from a
388 mixed community that are categorically lost in batch cultures under the same media conditions
389 (**Fig 4**). Therefore, developing, high-throughput enrichment and isolation methods like
390 GrowMiDE + DE-FACS that do not favor fast-growing microorganisms might serve as a novel
391 approach to combat ‘The Great Plate Count Anomaly’.

392

393

394 **Acknowledgments**

395 We thank H. Bachmann for the *L. lactis* strains NZ9000 and NZ9010, and A. Maheshwari
396 for the *E. coli*-GFP strain. We also thank members of the Fordyce lab Dropception team and Prof.
397 A. Bhatt’s lab for helpful discussions on experiments. This work was supported in part by the US
398 National Science Foundation through the Center for Deep Dark Energy Biosphere Investigations,
399 N.I.H. 1DP2 GM123641 awarded to P.M.F, and a Simons Postdoctoral Fellowship in Marine
400 Microbial Ecology to A. L. McCully from the Simons Foundation, Division of Life Sciences,
401 award #600755. P.M.F. is a Chan Zuckerberg Biohub Investigator.

402

403 **Data Availability Statement:**

404 All raw data and Matlab scripts are freely available to any researcher upon request. 16S sequencing
405 data has been submitted to SRA under BioProject PRJNA852267.

406

407 **References**

- 408 1. Pfeiffer T, Schuster S, Bonhoeffer S. Cooperation and competition in the evolution of
409 ATP-producing pathways. *Science (80-)* 2001; **293**: 1436.
- 410 2. Kreft JU. Biofilms promote altruism. *Microbiology* 2004; **150**: 2751–2760.
- 411 3. Weissman JL, Hou S, Fuhrman JA. Estimating maximal microbial growth rates from
412 cultures, metagenomes, and single cells via codon usage patterns. *Proc Natl Acad Sci U S*
413 *A* 2021; **118**: 1–10.
- 414 4. Roller BRK, Schmidt TM. The physiology and ecological implications of efficient
415 growth. *ISME J* 2015; **9**: 1481–1487.
- 416 5. Gray DA, Dugar G, Gamba P, Strahl H, Jonker MJ, Hamoen LW. Extreme slow growth as
417 alternative strategy to survive deep starvation in bacteria. *Nat Commun* 2019; **10**: 1–12.
- 418 6. Jørgensen BB, Marshall IPG. Slow Microbial Life in the Seabed. *Ann Rev Mar Sci* 2016;
419 **8**: 311–332.
- 420 7. Lever MA. Acetogenesis in the energy-starved deep biosphere-a paradox? *Front*
421 *Microbiol* 2012; **2**: 1–18.
- 422 8. Lloyd KG, Bird JT, Buongiorno J, Deas E, Kevorkian R, Noordhoek T, et al. Evidence for
423 a Growth Zone for Deep-Subsurface Microbial Clades in Near-Surface Anoxic Sediments.
424 *Appl Environ Microbiol* 2020; **86**.

- 425 9. Schut F, Quang P, Martin R, Robertson BR. Viability and Isolation of Marine Bacteria by
426 Dilution Culture : Theory , Procedures , and Initial Results. 1993; **59**: 881–891.
- 427 10. Mahler L, Niehs SP, Martin K, Weber T, Scherlach K, Hertweck C, et al. Highly
428 parallelized droplet cultivation and prioritization on antibiotic producers from natural
429 microbial communities. *Elife* 2021; **10**: 1–23.
- 430 11. Watterson WJ, Tanyeri M, Watson AR, Cham CM, Shan Y, Chang EB, et al. Droplet-
431 based high-throughput cultivation for accurate screening of antibiotic resistant gut
432 microbes. *Elife* 2020; **9**: 1–22.
- 433 12. Liu W, Kim HJ, Lucchetta EM, Du W, Ismagilov RF. Isolation, incubation, and parallel
434 functional testing and identification by FISH of rare microbial single-copy cells from
435 multi-species mixtures using the combination of chemistode and stochastic
436 confinementY. *Lab Chip* 2009; **9**: 2153–2162.
- 437 13. Grodrian A, Metze J, Henkel T, Martin K, Roth M, Köhler JM. Segmented flow
438 generation by chip reactors for highly parallelized cell cultivation. *Biosens Bioelectron*
439 2004; **19**: 1421–1428.
- 440 14. Villa MM, Bloom RJ, Silverman JD, Durand HK, Jiang S, Wu A, et al. Interindividual
441 Variation in Dietary Carbohydrate Metabolism by Gut Bacteria Revealed with Droplet
442 Microfluidic Culture. *mSystems* 2020; **5**: 1–17.
- 443 15. Kim HJ, Boedicker JQ, Choi JW, Ismagilov RF. Defined spatial structure stabilizes a
444 synthetic multispecies bacterial community. *Proc Natl Acad Sci U S A* 2008; **105**: 18188–
445 18193.

- 446 16. Churski K, Kaminski TS, Jakiela S, Kamysz W, Baranska-Rybak W, Weibel DB, et al.
447 Rapid screening of antibiotic toxicity in an automated microdroplet system. *Lab Chip*
448 2012; **12**: 1629–1637.
- 449 17. Huebner A, Olguin LF, Bratton D, Whyte G, Huck WTS, De Mello AJ, et al.
450 Development of quantitative cell-based enzyme assays in microdroplets. *Anal Chem* 2008;
451 **80**: 3890–3896.
- 452 18. Jarosz DF, Brown JCS, Walker GA, Datta MS, Ung WL, Lancaster AK, et al. Cross-
453 kingdom chemical communication drives a heritable, mutually beneficial prion-based
454 transformation of metabolism. *Cell* 2014; **158**: 1083–1093.
- 455 19. Terekhov SS, Smirnov I V., Stepanova A V., Bobik T V., Mokrushina YA, Ponomarenko
456 NA, et al. Microfluidic droplet platform for ultrahigh-throughput single-cell screening of
457 biodiversity. *Proc Natl Acad Sci U S A* 2017; **114**: 2550–2555.
- 458 20. Zengler K, Zaramela LS. The social network of microorganisms – how auxotrophies
459 shape complex communities. *Nat Rev Microbiol* 2018; In press.
- 460 21. Terekhov SS, Smirnov I V., Malakhova M V., Samoilov AE, Manolo AI, Nazarov AS, et
461 al. Ultrahigh-throughput functional profiling of microbiota communities. *Proc Natl Acad*
462 *Sci U S A* 2018; **115**: 9551–9556.
- 463 22. Park J, Kerner A, Burns MA, Lin XN. Microdroplet-enabled highly parallel co-cultivation
464 of microbial communities. *PLoS One* 2011; **6**.
- 465 23. Dichosa AEK, Daughton AR, Reitenga KG, Fitzsimons MS, Han CS. Capturing and
466 cultivating single bacterial cells in gel microdroplets to obtain near-complete genomes.

- 467 *Nat Protoc* 2014; **9**: 608–621.
- 468 24. Bachmann H, Fischlechner M, Rabbers I, Barfa N, Dos Santos FB, Molenaar D, et al.
469 Availability of public goods shapes the evolution of competing metabolic strategies. *Proc*
470 *Natl Acad Sci U S A* 2013; **110**: 14302–14307.
- 471 25. Baret JC, Miller OJ, Taly V, Ryckelynck M, El-Harrak A, Frenz L, et al. Fluorescence-
472 activated droplet sorting (FADS): Efficient microfluidic cell sorting based on enzymatic
473 activity. *Lab Chip* 2009; **9**: 1850–1858.
- 474 26. Cole RH, Tang SY, Siltanen CA, Shahi P, Zhang JQ, Poust S, et al. Printed droplet
475 microfluidics for on demand dispensing of picoliter droplets and cells. *Proc Natl Acad Sci*
476 *U S A* 2017; **114**: 8728–8733.
- 477 27. Brower KK, Khariton M, Suzuki PH, Still C, Kim G, Calhoun SGK, et al. Double
478 Emulsion Picoreactors for High-Throughput Single-Cell Encapsulation and Phenotyping
479 via FACS. *Anal Chem* 2020; **22**: 2020.06.07.139311.
- 480 28. Zhang Y, Ho Y-P, Chiu Y-L, Cham HF, Chlebina B, Schuhmann T, et al. A
481 programmable microenvironment for cellular studies via microfluidics-generated double
482 emulsions. *Biomaterials* 2013; **32**: 4564–4572.
- 483 29. Ong ILH, Amstad E. Selectively Permeable Double Emulsions. *Small* 2019; **15**: 1–12.
- 484 30. Etienne G, Vian A, Biočanin M, Deplancke B, Amstad E. Cross-talk between emulsion
485 drops: How are hydrophilic reagents transported across oil phases? *Lab Chip* 2018; **18**:
486 3903–3912.
- 487 31. Brower KK, Carswell-Crumpton C, Klemm S, Cruz B, Kim G, Calhoun SGK, et al.

- 488 Double emulsion flow cytometry with high-throughput single droplet isolation and nucleic
489 acid recovery. *Lab Chip* 2020; **20**: 2062–2074.
- 490 32. Lim SW, Abate AR. Ultrahigh-throughput sorting of microfluidic drops with flow
491 cytometry. *Lab Chip* 2013; **13**: 4563–4572.
- 492 33. Fodor AA, DeSantis TZ, Wylie KM, Badger JH, Ye Y, Hepburn T, et al. The ‘most
493 wanted’ taxa from the human microbiome for whole genome sequencing. *PLoS One* 2012;
494 **7**.
- 495 34. Goel A, Santos F, de Vos WM, Teusink B, Molenaar D. Standardized assay medium to
496 measure *Lactococcus lactis* enzyme activities while mimicking intracellular conditions.
497 *Appl Environ Microbiol* 2012; **78**: 134–143.
- 498 35. Dinh HT, Kuever J, Mußmann M, Hassel AW. Iron corrosion by novel anaerobic
499 microorganisms. *Nature* 2004; **427**: 829–832.
- 500 36. Goodman AL, Kallstrom G, Faith JJ, Reyes A, Moore A, Dantas G, et al. Extensive
501 personal human gut microbiota culture collections characterized and manipulated in
502 gnotobiotic mice. *Proc Natl Acad Sci U S A* 2011; **108**: 6252–6257.
- 503 37. Lohner ST, Deutzmann JS, Logan BE, Leigh J, Spormann AM. Hydrogenase-independent
504 uptake and metabolism of electrons by the archaeon *Methanococcus maripaludis*. *ISME J*
505 2014; **8**: 1673–1681.
- 506 38. Holtze C, Rowat AC, Agresti JJ, Hutchison JB, Angilè FE, Schmitz CHJ, et al.
507 Biocompatible surfactants for water-in-fluorocarbon emulsions. *Lab Chip* 2008; **8**: 1632–
508 1639.

- 509 39. Meyer JS, Tsuchiya HM. Dynamics of Mixed Populations Having Complementary
510 Metabolism. *Biotechnol Bioeng* 1975; **17**: 1065–1081.
- 511 40. Lee IH, Fredrickson AG, Tsuchiya HM. Dynamics of mixed cultures of *Lactobacillus*
512 *plantarum* and *Propionibacterium shermanii*. *Biotechnol Bioeng* 1976; **18**: 513–26.
- 513 41. Greenblum S, Turnbaugh PJ, Borenstein E. Metagenomic systems biology of the human
514 gut microbiome reveals topological shifts associated with obesity and inflammatory bowel
515 disease. *Proc Natl Acad Sci U S A* 2012; **109**: 594–599.
- 516 42. Rowland I, Gibson G, Heinken A, Scott K, Swann J, Thiele I, et al. Gut microbiota
517 functions: metabolism of nutrients and other food components. *Eur J Nutr* 2018; **57**: 1–24.
- 518 43. Rodionov DA, Arzamasov AA, Khoroshkin MS, Iablokov SN, Leyn SA, Peterson SN, et
519 al. Micronutrient requirements and sharing capabilities of the human gut microbiome.
520 *Front Microbiol* 2019; **10**: 1–22.
- 521 44. Tramontano M, Andrejev S, Pruteanu M, Klünemann M, Kuhn M, Galardini M, et al.
522 Nutritional preferences of human gut bacteria reveal their metabolic idiosyncrasies. *Nat*
523 *Microbiol* 2018; **3**: 514–522.
- 524 45. Diakite A, Dubourg G, Dione N, Afouda P, Bellali S, Ngom II, et al. Optimization and
525 standardization of the culturomics technique for human microbiome exploration. *Sci Rep*
526 2020; **10**: 9674.
- 527 46. Wu F, Guo X, Zhang J, Zhang M, Ou Z, Peng Y. *Phascolarctobacterium faecium*
528 abundant colonization in human gastrointestinal tract. *Exp Ther Med* 2017; **14**: 3122–
529 3126.

- 530 47. Del Dot T, Osawa R, Stackebrandt E. *Phascolarctobacterium faecium* gen. nov, spec. nov.,
531 a Novel Taxon of the Sporomusa Group of Bacteria. *Syst Appl Microbiol* 1993; **16**: 380–
532 384.
- 533 48. Watanabe Y, Nagai F, Morotomi M. Characterization of *Phascolarctobacterium*
534 *succinatutens* sp. Nov., an asaccharolytic, succinate-utilizing bacterium isolated from
535 human feces. *Appl Environ Microbiol* 2012; **78**: 511–518.
- 536 49. Ikeyama N, Murakami T, Toyoda A, Mori H, Iino T, Ohkuma M, et al. Microbial
537 interaction between the succinate-utilizing bacterium *Phascolarctobacterium faecium* and
538 the gut commensal *Bacteroides thetaiotaomicron*. *Microbiologyopen* 2020; **9**: 1–14.
- 539 50. Bernath K, Hai M, Mastrobattista E, Griffiths AD, Magdassi S, Tawfik DS. In vitro
540 compartmentalization by double emulsions: Sorting and gene enrichment by fluorescence
541 activated cell sorting. *Anal Biochem* 2004; **325**: 151–157.
- 542 51. Zinchenko A, Devenish SRA, Kintsjes B, Colin PY, Fischlechner M, Hollfelder F. One in
543 a million: Flow cytometric sorting of single cell-lysate assays in monodisperse picolitre
544 double emulsion droplets for directed evolution. *Anal Chem* 2014; **86**: 2526–2533.
- 545 52. Sidore AM, Lan F, Lim SW, Abate AR. Enhanced sequencing coverage with digital
546 droplet multiple displacement amplification. *Nucleic Acids Res* 2015; **44**: 1–9.
- 547 53. Boedicker JQ, Li L, Kline TR, Ismagilov RF. Detecting bacteria and determining their
548 susceptibility to antibiotics by stochastic confinement in nanoliter droplets using plug-
549 based microfluidics. *Lab Chip* 2008; **8**: 1265–1272.
- 550 54. Kintsjes B, Hein C, Mohamed MF, Fischlechner M, Courtois F, Lainé C, et al. Picoliter

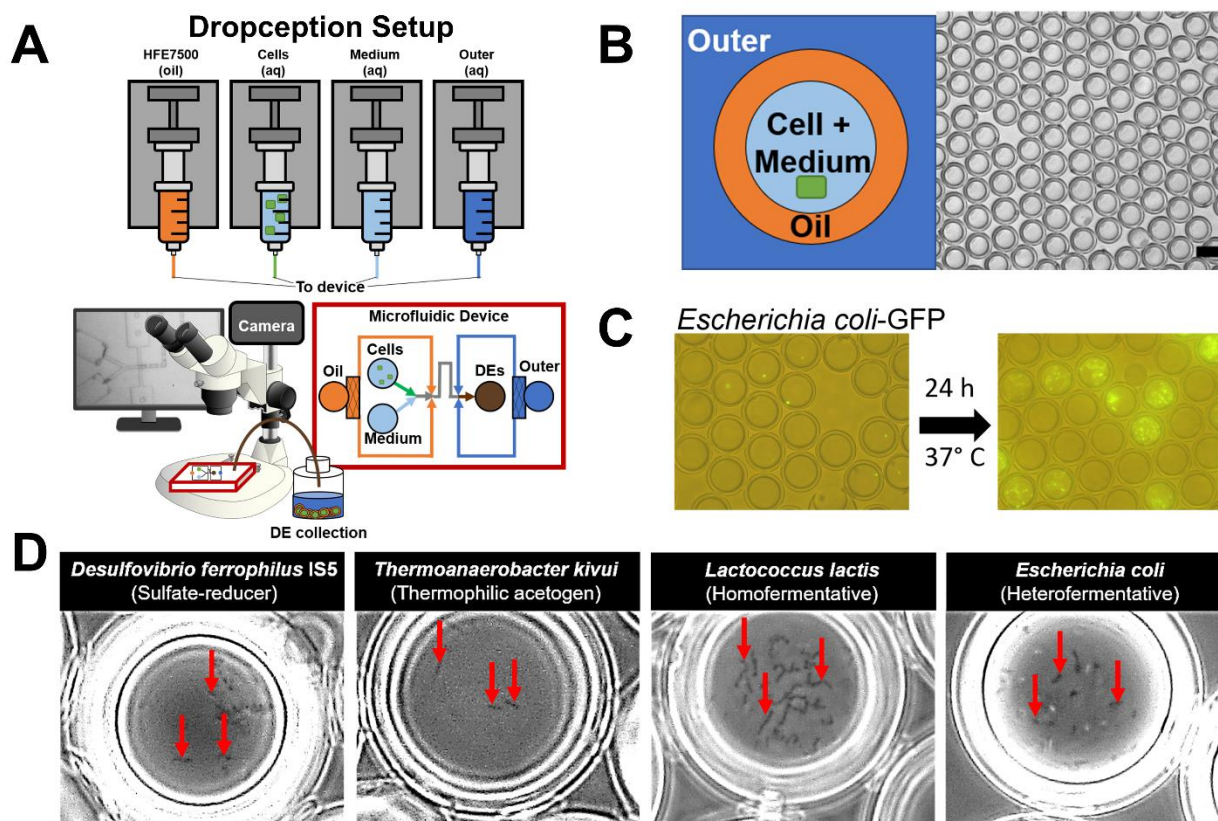
- 551 cell lysate assays in microfluidic droplet compartments for directed enzyme evolution.
552 *Chem Biol* 2012; **19**: 1001–1009.
- 553 55. Sukovich DJ, Lance ST, Abate AR. Sequence specific sorting of DNA molecules with
554 FACS using 3dPCR. *Sci Rep* 2017; **7**: 1–9.
- 555 56. Ho TM, Razzaghi A, Ramachandran A, Mikkonen KS. Emulsion characterization via
556 microfluidic devices: A review on interfacial tension and stability to coalescence. *Adv*
557 *Colloid Interface Sci* 2022; **299**: 102541.
- 558 57. Estrela S, Morris JJ, Kerr B. Private benefits and metabolic conflicts shape the emergence
559 of microbial interdependencies. *Environ Microbiol* 2016; **18**: 1415–1427.
- 560 58. Celiker H, Gore J. Competition between species can stabilize public-goods cooperation
561 within a species. *Mol Syst Biol* 2012; **8**: 1–9.
- 562 59. McCully AL, LaSarre B, McKinlay JB. Recipient-biased competition for an intracellularly
563 generated cross-fed nutrient is required for coexistence of microbial mutualists. *MBio*
564 2017; **8**: e01620-17.
- 565 60. Ogata Y, Suda W, Ikeyama N, Hattori M, Ohkuma M, Sakamoto M. Complete Genome
566 Sequence of *Phascolarctobacterium faecium* JCM 30894, a Succinate-Utilizing Bacterium
567 Isolated from Human Feces. *Microbiol Resour Announc* 2019; **8**: e01487-18.
- 568 61. Nichols D, Cahoon N, Trakhtenberg EM, Pham L, Mehta A, Belanger A, et al. Use of
569 Ichip for High-Throughput In Situ Cultivation of “Uncultivable ” Microbial Species □.
570 *Appl Environ Microbiol* 2010; **76**: 2445–2450.
- 571 62. Du W, Li L, Nichols KP, Ismagilov RF. SlipChip. *Lab Chip* 2009; **9**: 2286–2292.

572 63. Ma L, Kim J, Hatzenpichler R, Karymov MA, Hubert N, Hanan IM, et al. Gene-targeted
573 microfluidic cultivation validated by isolation of a gut bacterium listed in human
574 microbiome project's most wanted taxa. *Proc Natl Acad Sci U S A* 2014; **111**: 9768–9773.

575

576

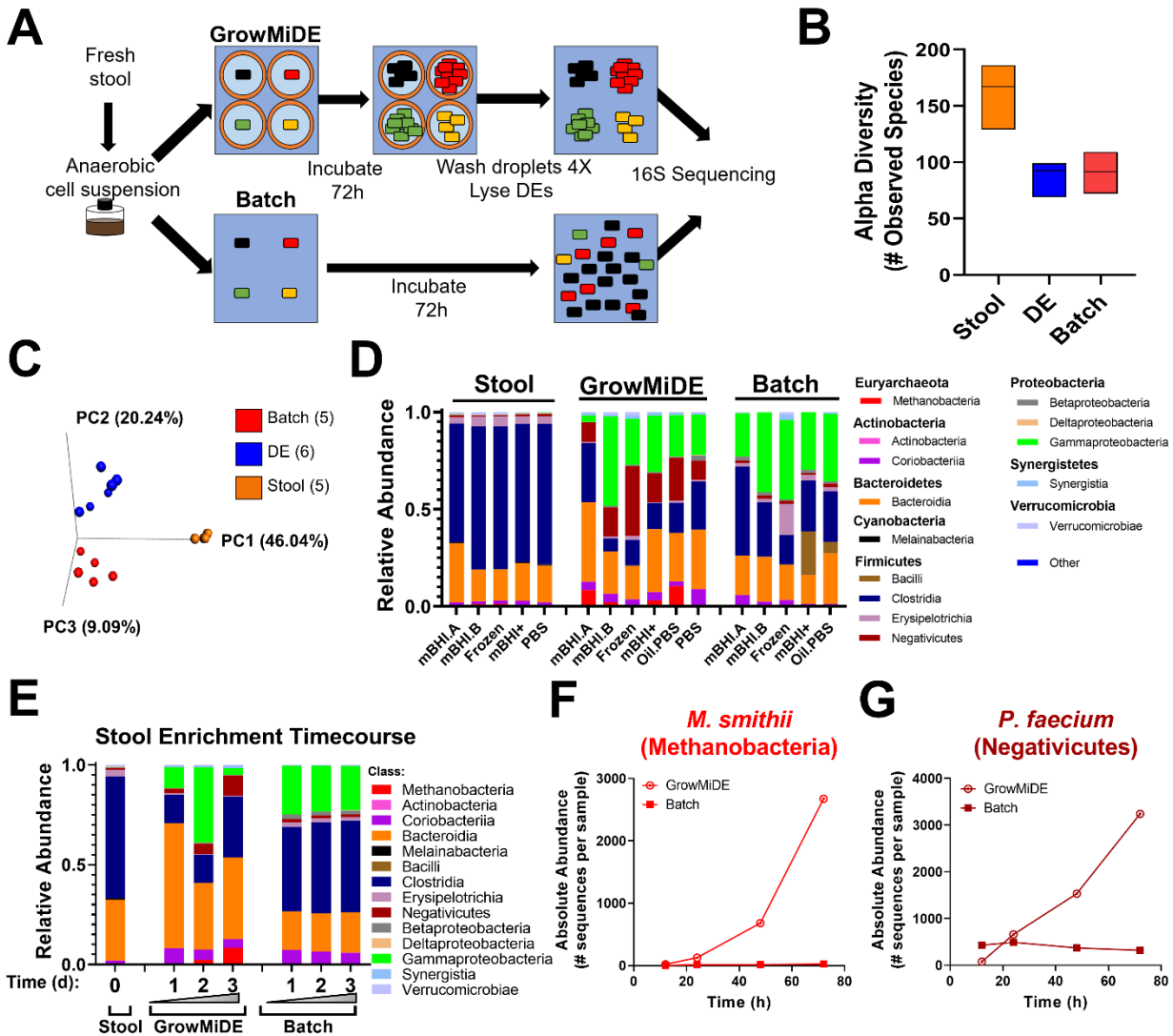
577 **Figures and Tables**



578

579 **Figure 1. GrowMiDE: Double emulsion platform for bacterial cultivation.** (A) Schematic representation of the
580 GrowMiDE platform. Four syringe pumps drive oil and aqueous solutions into a custom microfluidic device to
581 encapsulate single microbes within 30 or 45 μm diameter double emulsions (DEs); DE generation is monitored in
582 real-time by a high-speed camera attached to an Amscope stereoscope. (B) Schematic and representative brightfield
583 image of DE droplets. (C) Merged brightfield and fluorescent images of single *E. coli*-GFP cells loaded into DEs (left)
584 and after growth in M9 + glucose for 24 hours (right). (D) Brightfield microscopy images indicating growth of diverse
585 anaerobes within DEs including the sulfate-reducer *Desulfovibrio ferrophilus* IS5 on 60 mM lactate and 30 mM
586 NaSO_4 , the acetogen *Thermoanaerobacter kivui* on 50 mM glucose at 65°C, lactic acid-producing fermenter
587 *Lactococcus lactis* NZ9000 on 50 mM glucose, and mixed acid fermenter *E. coli* MG1655 on 50 mM glucose.

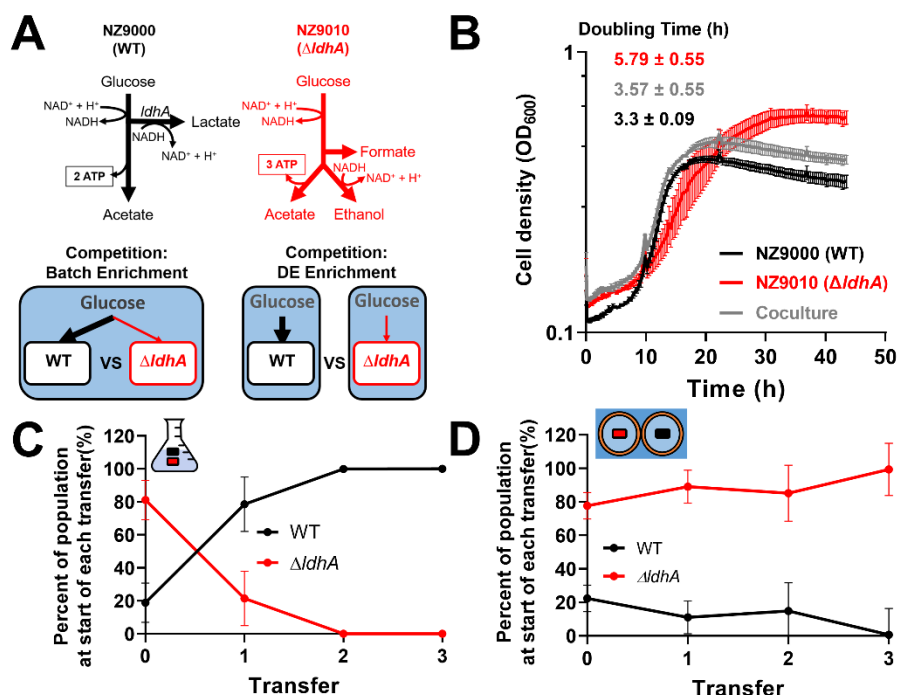
588



589

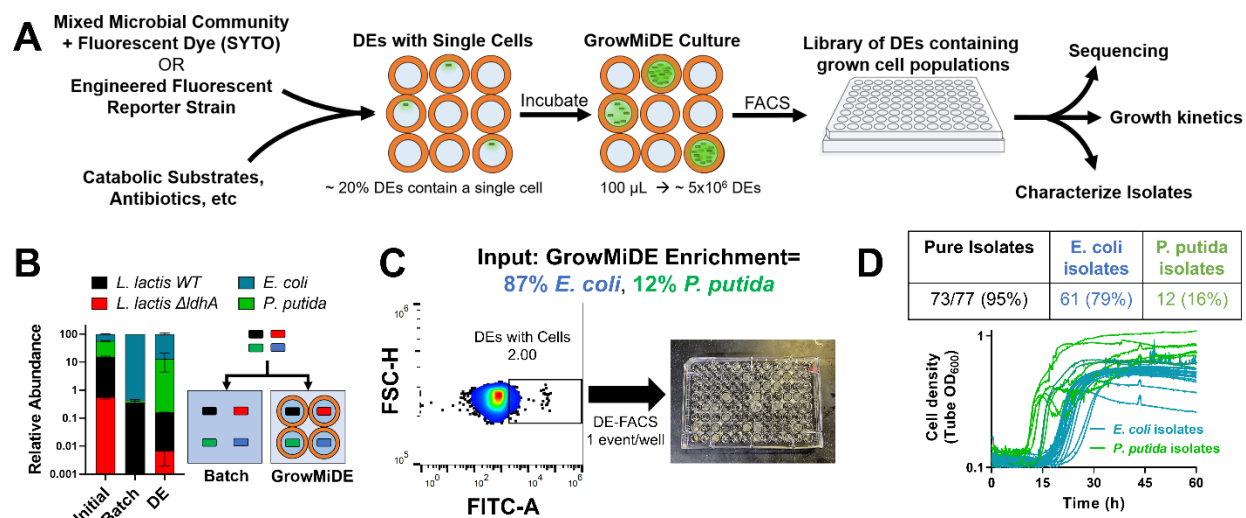
590 **Figure 2. GrowMiDE enrichment of distinct microbial communities from human gut microbiota.** (A) Schematic
 591 overview of stool enrichments in DEs vs batch enrichments in mBHI. (B) Alpha diversity from input stool,
 592 GrowMiDE, and batch enrichments based on total unique ASVs. Floating bar plots represent the mean and range,
 593 n=5-6. (C) Beta diversity from input stool, GrowMiDE, and batch enrichments based on type of unique ASVs. (D)
 594 Relative 16S rRNA gene abundances from input stool samples, GrowMiDE enrichments, and batch enrichments from
 595 stool cell suspensions. (E) Relative 16S rRNA gene abundances from a timecourse of stool enrichments in DE vs
 596 batch cultures sacrificed at 12, 24, 48, and 72 hours, and corresponding absolute 16S rRNA gene abundances of (F)
 597 *M. smithii* (class: Methanobacteria) and (G) *P. faecium* (class: Negativicutes).

598



599

600 **Figure 3. GrowMiDE can maintain and enrich growth yield specialists through nutrient privatization. (A)**
 601 Fermentation pathways of *L. lactis* WT (black) and $\Delta ldhA$ (red) strains in mixed batch cultures or GrowMiDE
 602 enrichments. **(B)** Growth of *L. lactis* monocultures and cocultures (1:1 starting ratio) on CDM + 25 mM glucose (n =
 603 3, biological replicates, error bars indicate SEM). **(C)** Frequencies of populations across transfers in mixed batch
 604 cultures of *L. lactis* strains on 50 mM glucose. Each transfer received a 1% inoculum into fresh CDM + 50 mM
 605 glucose, and CFUs for each strain were determined from the grown community at each transfer (n = 3, biological
 606 replicates, error bars indicate SEM). **(D)** Cell densities across transfers in GrowMiDE enrichments of *L. lactis*
 607 on 50 mM glucose. Initial mixed culture contained ~80% $\Delta ldhA$ as determined by CFUs/mL on CDM + Ery⁵ plates.
 608 At the end of each transfer, the DEs were disrupted in bulk by incubating with 1H,1H,2H,2H-perfluoro-1-octanol
 609 (PFO), diluted to an OD = 0.05 to achieve single-cell loading, and cells were re-packaged into DEs for the next
 610 transfer. (n = 3, technical replicates, error bars indicate SEM). CFUs for each strain were determined from the grown
 611 community at each transfer to determine relative cell densities, and the initial mixed culture contained ~80% $\Delta ldhA$
 612 prior to splitting into batch or DE competition experiments. All *L. lactis* transfers were incubated for 48 hours at 30°C.
 613



614

615 **Figure 4. GrowMiDE + DE-FACS as a novel microbial enrichment and isolation platform. (A)** Overview and

616 potential applications for microbial enrichments using GrowMiDE followed by DE-FACS to obtain isolates. **(B)**

617 Relative ratios of 4 glucose-catabolizing strains in a mock community enriched in batch cultures or the GrowMiDE

618 platform on CDM + 25 mM glucose for 48 hours. n=3. Error bars indicate SEM. **(C)** FACS profiles of 30 μ m DEs

619 containing the mock community encapsulated with 2.5 μ M SYTO9 after 48 hours and subsequently sorted into

620 individual wells on a 96-well plate. Plate wells were preloaded with growth medium and 10uL of PFO to disrupt

621 DEs. 767 events were gated within the top 2% of the SYTO⁺ DE population (38321 events) and 192 were sorted

622 onto plates to assess for growth. **(D)** Growth curves of 34 representative output isolates downstream of DE-FACS.

623 All growth assays were performed at 30°C.

624